Electronic Supplementary Material (ESI) for Journal of Materials Chemistry C.

Supporting Information

An Organic-Inorganic Hybrid Co-crystal Complex as High Performance Solid-State Nonlinear Optical Switch

Tianliang Chen, Zhihua Sun,* Sangen Zhao, Chengmin Ji and Junhua Luo*

Key Laboratory of Optoelectronic Materials Chemistry and Physics, Fujian Institute of Research on the Structure of Matter, Chinese Academy of Sciences, Fuzhou 350002, China

Figure captions

Figure S1. The grown bulk crystals.

Figure S2. Powder X-ray diffraction pattern of **1**.

Figure S3. Differential scanning calorimetry of **1** at different rate (2, 5, 10 k/min, respectively), the intercept with straight line showing the feature of a second-order phase transition.

Figure S4. a) Packing diagram of **1** along *c*-axis at 293 K; b) Packing diagram of **1** along *a*-axis at 100 K.

Figure S5. a) The reorientation between the two neighboured [$FeCl_3(H_2O)_3$] octahedrons in the inorganic layer of **1** at 293K. The angle of the equatorial plane of the neighbor two [$FeCl_3(H_2O)_3$] octahedrons is 0; b) The reorientation between the two neighboured [$FeCl_3(H_2O)_3$] octahedrons in the inorganic layer of **1** at 100K. The angle of the equatorial plane of the neighbor two [$FeCl_3(H_2O)_3$] octahedrons is 7.23º.

Figure S6. Diffuse reflection spectrum of **1** measured in the range of 400-1800 nm.

Figure S7. SHG intensity for 1 as a function of particle size at 160 K.

Figure S8- S9. Analysis of the molecular dipole moments.

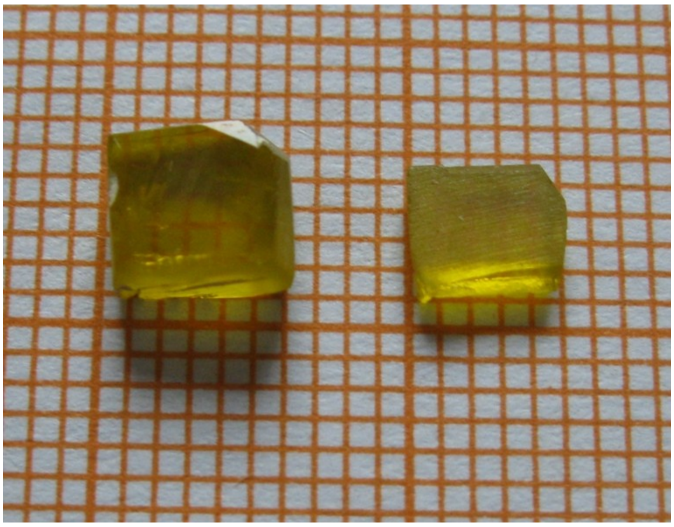

Figure S1. The grown bulk crystals**.**

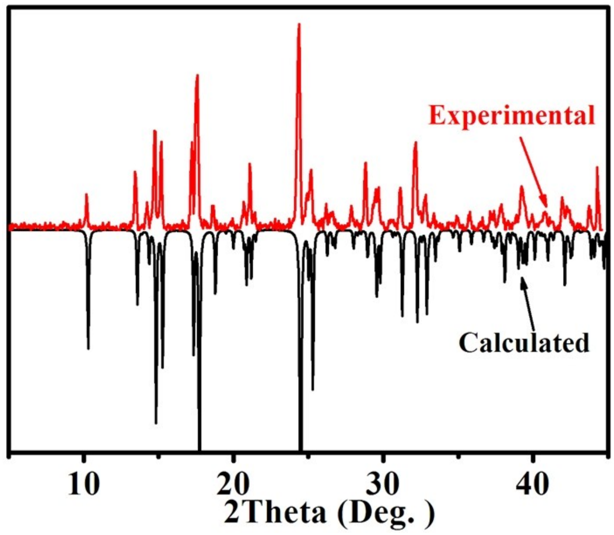

Figure S2. Powder X-ray diffraction pattern of **1**

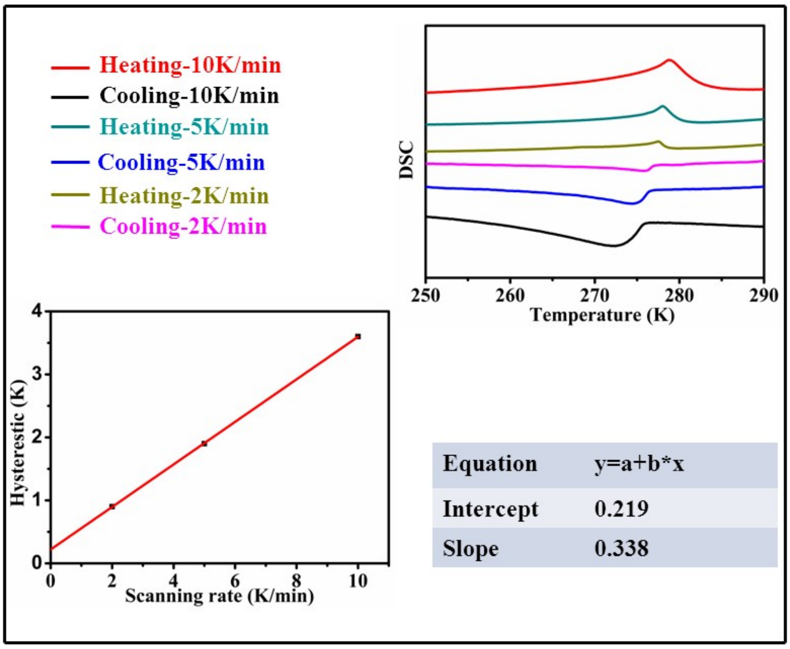

Figure S3. Differential scanning calorimetry of **1** at different rate (2, 5, 10 k/min, respectively), the intercept with straight line showing the feature of a second-order phase transition.

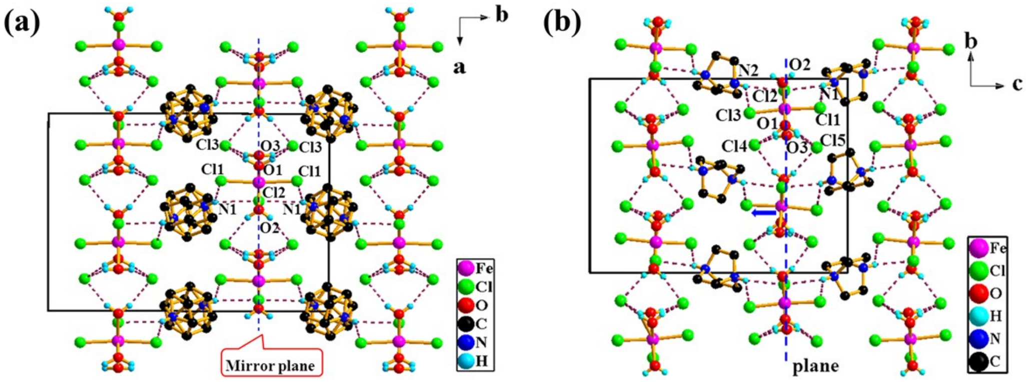

Figure S4. a) Packing diagram of **1** along *c*-axis at 293 K; b) Packing diagram of **1** along *a*-axis at 100 K.

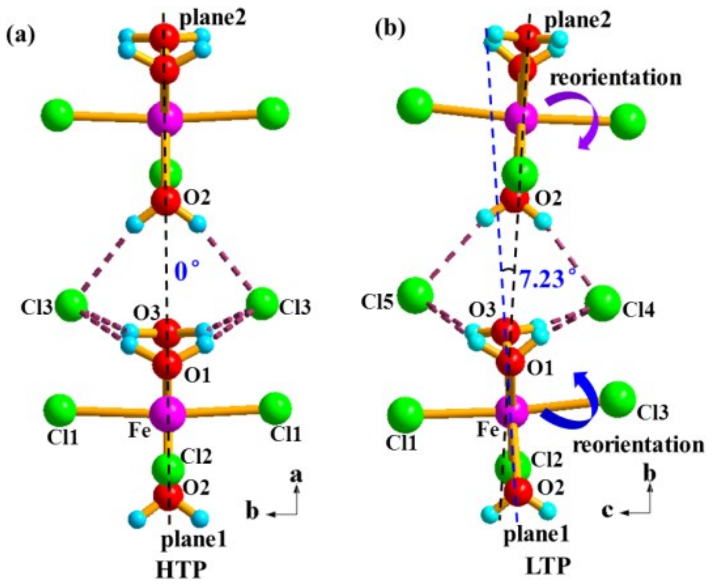

Figure S5. a) The reorientation between the two neighboured [$FeCl_3(H_2O)_3$] octahedrons in the inorganic layer of **1** at 293K. The angle of the equatorial plane of the neighbor two [$FeCl_3(H_2O)_3$] octahedrons is 0; b) The reorientation between the two neighboured [$FeCl_3(H_2O)_3$] octahedrons in the inorganic layer of **1** at 100K. The angle of the equatorial plane of the neighbor two [$FeCl_3(H_2O)_3$] octahedrons is 7.23º.

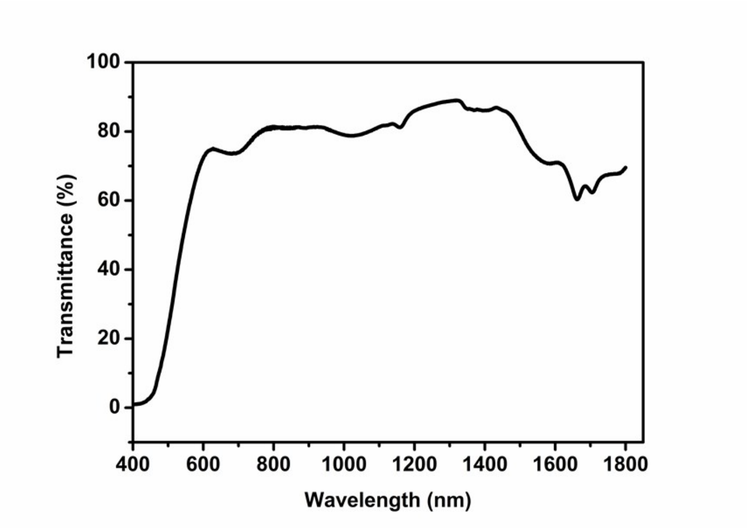

Figure S6. Diffuse reflection spectrum of **1** measured in the range of 400-1800 nm.

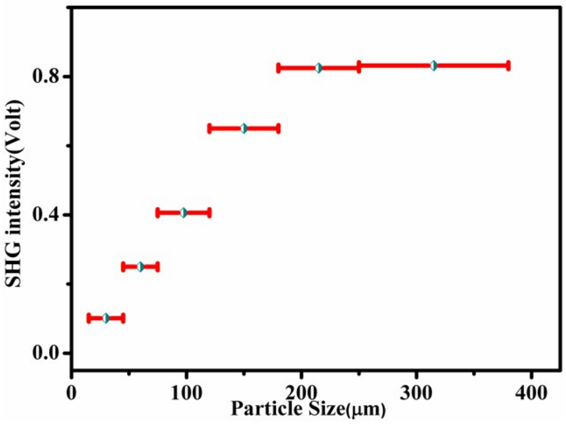

Figure S7. SHG intensity for 1 as a function of particle size at 160 K.

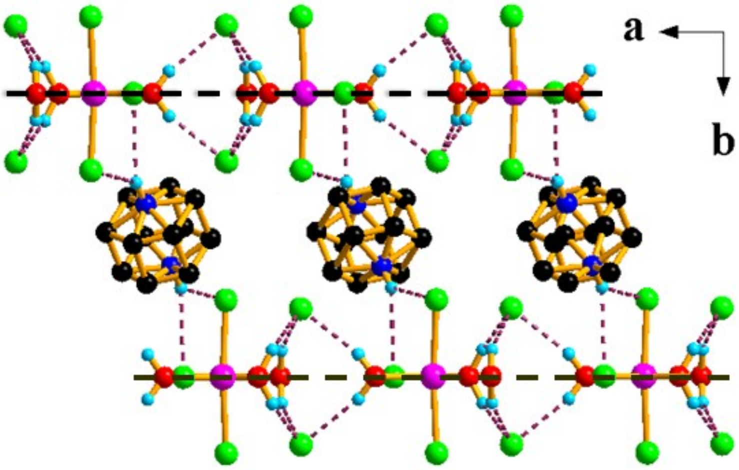

Figure S8. Crystal structure of unit cell for **1** in the "SHG-OFF" state viewed from the [001] direction. For the organic H_2dabco·2Cl component, C and N atoms are located in their disordered sites according to the symmetry requirements. The average protonated N atoms of the dabco cation are located (0.5, 0.5, 0.5) and the average uncoordinated Cl atom are located (0.5, 0.5, 0.5). We assume that the dipole centers are located at the average protonated N and uncoordinated Cl atoms. Accordingly, the molecular dipolar moments of organic species are zero. The inorganic $[FeCl_3(H_2O)_3]$ component are located in the symmetric mirror plane. The coordinate of the Fe atom and Cl2 atom are Y_i= 0.25 or 0.75. We assume that the dipole centers are located at the Fe and Cl2 atom. Consequently, the molecular dipolar moments of inorganic species are also zero.

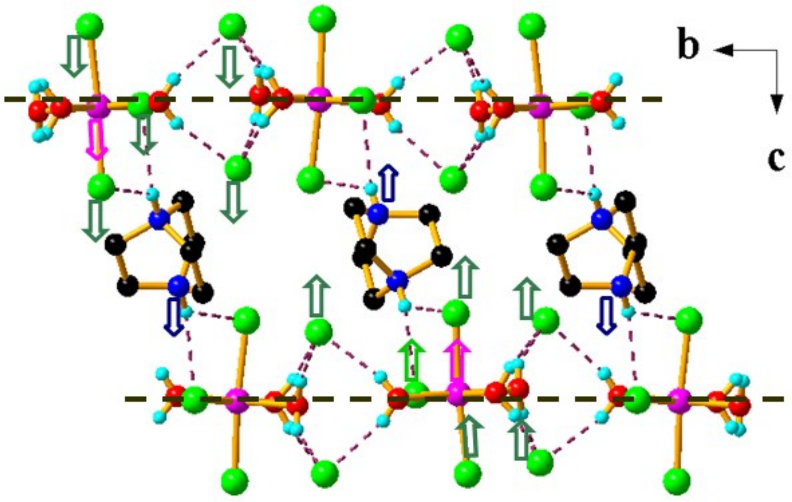

Figure S9. Crystal structure of unit cell for **1** in the "SHG-ON" state viewed from the [100] direction. One can clearly see all atoms have been determined in the definitive sites. The average N atom of the dabco cation and the average two uncoordinated Cl atom (Cl4 and Cl5 atom) along *c*-axis is 0.4954 and 0.5096. Therefore, their displacements are -0.0046 × |b| and 0.0096 × |b|, respectively. In addition, the coordinates of four Fe atoms along *c*-axis are 0.7439, 0.2439, 0.2561 and 0.7561, respectively; the coordinates of four Cl2 atoms along *c*-axis are 0.6072, 0.1072, 0.3928 and 0.8928, respectively. Thus, their displacements are -0.0061 × |b| and -0.1428 × |b|, respectively. Although the total polarity of **1** is zero since it crystallizes in the nonpolar space group $P2_12_12_1$, the molecular dipole moment (μ) of the organic H_2dabco·2Cl component and inorganic $[FeCl_3(H_2O)_3]$ component along its *c*-axis (in LTP) can be approximately estimated to be:

μ(organic component) = (0.0096+0.0046) × 2 × 16.9517 × 10^{-10} m × 1.6×10^{-19} C = 0.716 × 10^{-29} C·m

μ(inorganic component) = (-0.1428+0.0061) × 3× 16.9517 × 10^{-10} m × 1.6×10^{-19} C = -11.1× 10^{-29} C·m

μ(molecule of **1**) = 0.716 × 10^{-29} C·m + (-11.1× 10^{-29} C·m) = -10.3 × 10^{-29} C·m

Table S1. Crystal Data and structure refinement of **1** at 100 K and 293 K

Temperature (K)	293(2)	100(2)
Moiety formula	$C_6H_8Cl_5FeN_2O_3$	$C_6H_8Cl_5FeN_2O_3$
Formula weight	401.34	401.34
Crystal system	Orthorhombic	Orthorhombic
Space group	*Pnma*	$P2_12_12_1$
a/Å	12.7268(6)	6.9337(2)
b/Å	17.1535(7)	12.7285(4)
c/Å	7.0352(3)	16.9517(7)
Volume (Å^3)	1535.85(12)	1524.67 (3)
Z	4	4
F(000)	772.0	820.0
Goodness-of-fit on F^2	1.045	1.135
R_1 (on F_o^2, $I>2\sigma(I)$)	0.0421	0.0321
wR_2 (on F_o^2, $I>2\sigma(I)$)	0.1272	0.0834

$\alpha R_1 = \Sigma||F_o| - |F_c||/\Sigma|F_o|$, $wR_2 = [\Sigma(|F_o|^2 - |F_c|^2) / \Sigma|F_o|^2]^{1/2}$

Table S2 The bond lengths and bond angles of the octahedron [$FeCl_3(H_2O)_3$] of **1** in HTP

Bonds	Bond angle	Bonds	Bond lengths
O3–Fe(1) –O1	90.429°	Fe(1) –O1	2.0662 Å
O3–Fe(1) –O2	179.468°	Fe(1) –O2	2.0564 Å
O3–Fe(1) –Cl1	90.055°	Fe(1) –O3	2.0456 Å
O3–Fe(1) –Cl2	89.334°	Fe(1) –Cl1	2.3292 Å
O2–Fe(1) –O1	90.103°	Fe(1) –Cl2	2.3268 Å
O2–Fe(1) –Cl1	89.99°		
O2–Fe(1) –Cl2	90.134°		
Cl1–Fe(1) –Cl3	170.286°		

Table S3 The bond lengths and bond angles of the octahedron [$FeCl_3(H_2O)_3$] of **1** in LTP.

Bonds	Bond angle	Bonds	Bond lengths
O3–Fe(1) –O1	90.576°	Fe(1) –O1	2.0600 Å
O3–Fe(1) –O2	179.277°	Fe(1) –O2	2.0476 Å
O3–Fe(1) –Cl1	91.173°	Fe(1) –O3	2.0436 Å
O3–Fe(1) –Cl2	89.503°	Fe(1) –Cl1	2.3319 Å
O3–Fe(1) –Cl3	89.575°	Fe(1) –Cl2	2.3350 Å
O2–Fe(1) –O1	90.108°	Fe(1) –Cl3	2.3292 Å
O2–Fe(1) –Cl1	89.122°		
O2–Fe(1) –Cl2	89.814°		
O2–Fe(1) –Cl3	90.246°		
Cl1–Fe(1) –Cl3	170.21°		